Ore fluid geochemistry of the Jinlongshan Carlin-type gold ore belt in Shaanxi Province, China*

ZHANG Jing (张 静)[1,2], CHEN Yanjing (陈衍景)[2,3**], ZHANG Fuxin (张复新)[4], and LI Chao (李 超)[2]

[1] *State Key laboratory of Geological Processes and Mineral Resources, China University of Geosciences, Beijing* 100083, *China*
[2] *Laboratory of Crust and Orogen Evolution, Peking University, Beijing* 100871, *China*
[3] *Institute of Geochemistry, Chinese Academy of Sciences, Guiyang* 550002, *China*
[4] *Department of Geology, Northwest University, Xi'an* 710069, *China*

Abstract The Jinlongshan gold ore belt in southern Shaanxi Province contains a number of Carlin-type gold deposits in the Qinling collisional orogenic belt. Their fluid inclusions are of the $Na^+ - Cl^-$ type. From the main metallogenic stage to later stages, the total quantity of anions and cations, temperature and deoxidation parameter (R) for fluid inclusions all gradually decreased, suggesting the gradual intensification of fluid oxidation, the reduction of metallogenic depth and the input of meteoric water and organic components. The deposits were formed during crustal uplifting and hence had similar tectonic settings to orogenic gold deposits. The CO_2 contents and CO_2/H_2O values of the ore fluid increased from early to late stages, and the wall-rock alteration is represented by decarbonation, which is inconsistent with the characteristics of orogenic gold deposits. It is also discovered that Na^+, K^+, SO_4^{2-}, Cl^- and the total amounts of anions and cations in the inclusions in quartz are higher than those in the coexisting calcite. The H, O and C isotope ratios indicate that the ore fluid was sourced from meteoric water and metamorphic devolatilisation of the sedimentary rocks that host the ores. The high background $\delta^{18}O$ and $\delta^{13}C$ values of wall rocks resulted in high $\delta^{18}O$ and $\delta^{13}C$ values of ore fluid and also high $\delta^{18}O$ and $\delta^{13}C$ values of hydrothermal minerals such as quartz and carbonate. The carbon in ore fluid stemmed largely from the hosting strata. The $\delta^{18}O$ and $\delta^{13}C$ values of Fe-calcite and the δD values of fluid inclusions are lower than those of calcite and quartz. In terms of the theory of coordination chemistry, all these differences can be ascribed to water-rock interaction in the same fluid system, instead, to the multi-source of ore fluid.

Key words ore fluid; Jinlongshan gold ore belt; Carlin-type gold deposit; isotope; fluid inclusion; Qinling Orogen

The Jinlongshan gold ore belt in Zhen'an County, southern Shaanxi Province, is located in the western Qinling gold province (No. 16 in Fig. 1; Chen Yanjing et al., 2004). It was discovered in the Devonian strata in the late 1980s). Its geological setting and metallogenic evolution are similar to those of orogenic gold deposits (Zhang Fuxin et al., 2000, 2001). The development of the gold ore belt and the spatial localization of orebodies are strictly controlled by lithologies of the strata and ductile-brittle shear zones (Zhang Fuxin et al., 1997). This gold ore belt is an ideal subject of study to shed light on the rules of fluid involvement in metallogenesis of the Carlin-type gold deposits. Nevertheless, little work has been done on its ore fluids, hampering our understanding of the metallogenic mechanism and rule of this ore belt. Therefore, this paper is aimed at providing more information in these aspects.

1 Regional and ore geology

According to Chen Yanjing et al. (2004), the western Qinling area is the second largest Carlin-type and Carlin-like gold province in the world. Unlike Nevada, USA, which is located in the back-arc Basin-and -Range region, the western Qinling gold province (WQGP) is inboard a continental collision orogen. The WQGP includes four tectonic units: from north to south, the southern margin of Sino-Korean craton, the northern Qinling orogenic belt, the southern Qinling orogenic belt and the Songpan foreland fold-and-thrust belt (Fig. 1). All the Carlin-type and Carlin-like gold deposits in the WQGP occur in the southern Qinling o-

ISSN 1000-9426
* Granted by the National Natural Science Foundation of China (Projects Nos. 49672119, 49972035, 40352003, and 40425006) and the Hundred Young Scientists Program of Chinese Academy of Sciences.
** Corresponding author, E-mail: yjchen@pku.edu.cn

rogenic belt and the Songpan foreland fold-and-thrust belt, and are mainly hosted in Devonian-Triassic strata. The country rocks are mainly carbonaceous fine clastic-chemical sediments, including calcareous sandstones, silty carbonates, shales and cherts, deposited in lagoon-shallow sea environments. Most of the gold deposits were formed in the period from Late Triassic to Early Cretaceous, with isotope ages clustering at 170 Ma.

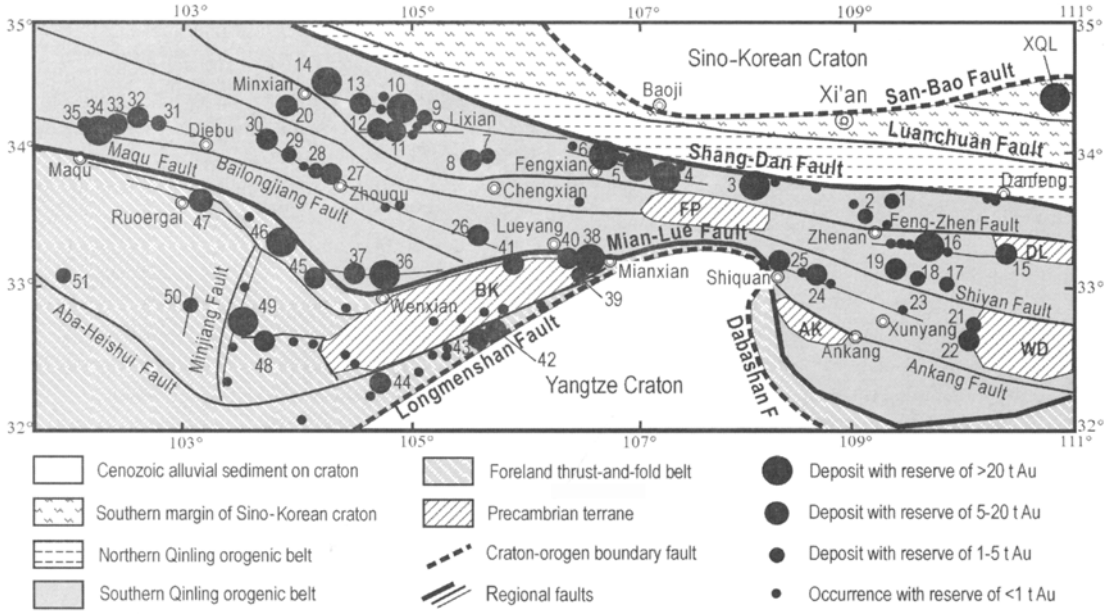

Fig. 1. Tectonic framework and gold distribution in the western Qinling gold province (modified from Chen Yanjing et al., 2004). Abbreviations: XQL. Xiaoqinling; AK. Ankang; FP. Foping; DL. Douling; WD. Wudang; BK. Bikou. Numbers of the deposits on the figure: 1. Xialiangzi, Zhashui, Shaanxi; 2. Ertaizi, Zhen'an, Shaanxi; 3. Ma'anqiao, Zhouzhi, Shaanxi; 4. Shuangwang, Taibai, Shaanxi; 5. Baguamiao, Fengxian, Shaanxi; 6. Pangjiahe, Fengxian, Shaanxi; 7. Xiaogouli, Xihe, Gansu; 8. Anjiacha, Xihe, Gansu; 9. Luoba, Lixian, Gansu; 10. Liba, Lixian, Gansu; 11. Maquan, Lixian, Gansu; 12. Jinshan, Lixian, Gansu; 13. Mingzhushan, Minxian, Gansu; 14. Zhaishang, Minxian, Gansu; 15. Xiajiadian, Shanyang, Shaanxi; 16. Jinglongshan, Zhen'an, Shaanxi; 17. Leishigou, Xunyang, Shaanxi; 18. Qingdonggou, Xunyang, Shaanxi; 19. Huijiagou, Xunyang, Shaanxi; 20. Lu'erba, Minxian, Gansu; 21. Xujiapo, Yunxian, Hubei; 22. Yindonggou, Yunxian, Hubei; 23. Linxiang, Xunyang, Shaanxi; 24. Huanglong, Hanying, Shaanxi; 25. Yangpingwan, Shiquan, Shaanxi; 26. Shangjiagou, Kangxian, Gansu; 27. Pingding, Zhouqu, Gansu; 28. Jiuyuan, Zhouqu, Gansu; 29. Lazikou, Diebu, Gansu; 30. Caibu, Diebu, Gansu; 31. Qiongmo, Zoigê, Sichuan; 32. La'erma, Luqu, Gansu; 33. Zhongqu, Luqu, Gansu; 34. Dashui, Maqu, Gansu; 35. Gongbei, Maqu, Gansu; 36. Yangshan, Wenxian, Gansu; 37. Shijiba, Wenxian, Gansu; 38. Jianchaling, Lueyang, Shaanxi; 39. Lijiagou, Mianxian, Shaanxi; 40. Donggouba, Lueyang, Shaanxi, 41. Huachanggou, Lueyang, Shaanxi; 42. Dingjianlin, Niangqiang, Shaanxi; 43. Taiyangping, Guangyuan, Sichuan; 44. Jindonggou, Pingwu, Sichuan; 45. Tuanjie, Nanping, Sichuan; 46. Manaoke, Nanping, Sichuan; 47. Baxi, Zoigê, Sichuan; 48. Qiaoqiaoshang, Songpan, Sichuan; 49. Dongbeizhai, Songpan, Sichuan; 50. Zheboshan, Songpan, Sichuan; 51. Jinmuda, Aba, Sichuan.

The Jinlongshan gold ore belt includes four gold deposits from east to west, i. e., Jinlongshan, Yaojian, Qiuling and Guloushan (Fig. 2), with total reserve > 30 t Au. According to Zhang Fuxin and Ma Jianqin (1996), Zhang Fuxin et al. (1997, 2000), the Jinlongshan gold ore belt occurs in the Zhen'an-Xunyang Late Paleozoic basin south of the Feng-Zhen fault (Fig. 1). Host rocks are the strata of the Upper Devonian Nanyangshan Formation and the Lower Carboniferous Yuanjiagou Formation (Fig. 2), of which the Nanyangshan Formation is the main ore-hosted stratum of gold deposits. The ore-bearing lithology commonly contains organic matter (Zhang Fuxin et al., 2000). Within the mining district (Fig. 2) nearly E-W extending faults are relatively developed, most of which possess thrusting characteristics, and they are controlled by the Zhen'an-Banyanzhen fault on the northern side. The southern and northern boundaries of the mining district are controlled by the second-ordered faults, i. e., the Miliang-Anjiamen and Qiuling-Potongya faults. The ore-controlling structures of the ore belt are ductile, ductile-brittle or brittle-shear zones

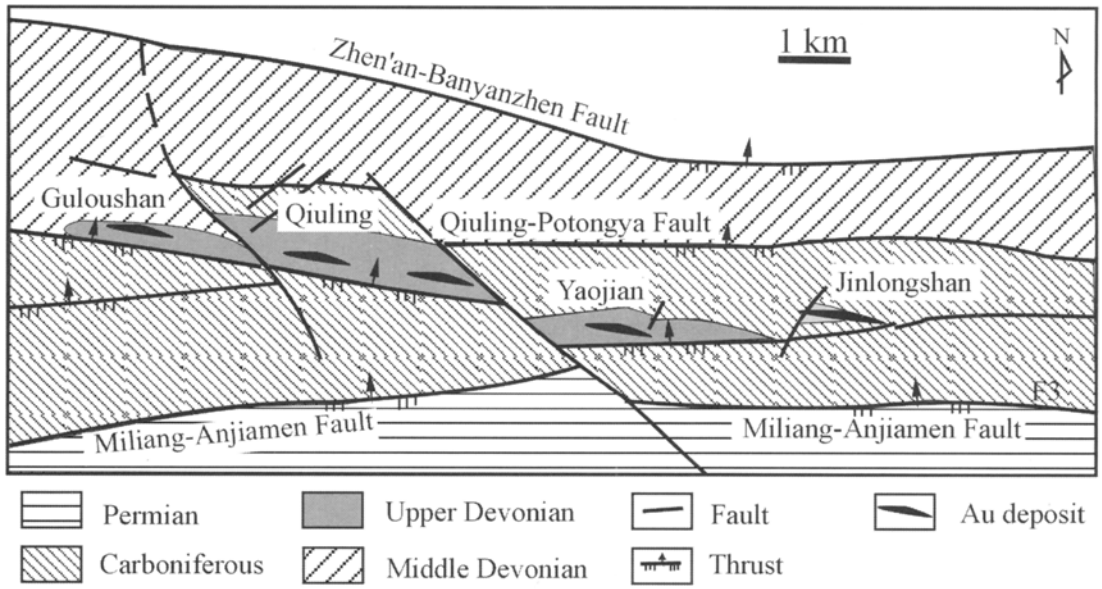

Fig. 2. Geological map of the Jinlongshan gold ore belt (modified from Hu Jianmin and Zhang Haishan, 1994).

(Zhang Fuxin and Ma Jianqin, 1996). In general, these shear zones axially overprint anticlines, constituting a kind of ore-hosting architecture usually called "anticline plus a cut" or "broken anticline". Therefore, combination of cleavages, which can pump ore fluids, and anticline hinges, which can trap fluids, resulted in intense hydrothermal alteration and gold mineralization in the Jinlongshan gold ore belt.

By combining our laboratory study and field observations, hydrothermal mineralization in the Jinlongshan gold ore belt can be divided into three main stages: 1) gold mineralization stage: the mineralization of auriferous pyrite was accompanied with sericitization, fine-grained silicification, decarbonation and arsenopyritization; the contents of Fe, As and Au were greatly increased; 2) Sb mineralization stage: this stage is characterized by the formation of stibnite-cinnabar assemblage, accompanied with the formation of quartz-calcite veins; and 3) carbonation stage: fine carbonate veinlets filled in fractures or tensional structures; miarolitic and comb structures are commonly observed; in the veinlets the contents of Au, As and Sb are relatively low, implying that this stage contributed little to gold mineralization. This work puts the focus on the fluid inclusion characteristics, chemical compositions and isotopic characteristics of quartz, calcite and other minerals formed during these three stages.

2 Fluid inclusion geochemistry

2.1 Petrography and microthermometry

In light of microscopic observations (Table 1), fluid inclusions in the Jinlongshan gold ore belt are relatively developed, but they are small in size, mostly less than 5 μm and generally between 1 – 3 μm. From the gold mineralization stage through the Sb mineralization stage to the carbonation stage the fluid inclusions tend to increase progressively in size and are dominated by liquid- and vapor/liquid-phase ones, with the V/L ratios varying between 5% and 25%. The fluid inclusions are mostly spheroid, elliptical, elongated and irregular in shape. Under microscope (40 × 10) one can observe many vapor-phase inclusions like tiny black dots jumping in liquid-phase inclusions. The homogenization temperatures of fluid inclusions trapped in the gold-mineralization stage range from 158 to – 268 ℃, mostly within the range of 180 – 220 ℃. The salinities [W (NaCleq)] vary between 5.7% and 7.9% (Zhang Fuxin et al., 1997). Homogenization temperatures for the Sb-mineralization stage range from 120 to 277 ℃, clustering in the span of 140 – 220 ℃. The salinities range from 8.3% to 8.6% (Zhang Fuxin et al., 1997). The homogenization temperatures for late-stage mineralization are within the range of 81 – 184 ℃, mostly within the range of 130 – 180 ℃. This indicates that from the Au-mineralization stage to the late carbonation stage, the temperatures decreased progressively, and the medium-low temperatures and medium-low salinities of the ore fluids are just in accord with the characteristics of the Carlin-type gold deposits.

Table 1. Microthermometric data of fluid inclusions from the Jinlongshan gold ore belt

Ore deposit mineralization	Sample No.	Host mineral	Inclusion shape	Size (μm)	V/(V+L) (%)	Homogenization temperature (℃)
Jinlongshan						
Au mineralization	J153-2	Q	Spheroid, irregular	1-5	6-30	158, 199, 207
Sb mineralization	J-PD7-Ca	Cc	Irregular, elliptic	1-3	10-20	151, 218, 246
Carbonation	J131, J138, J-mg-1, -2, -5	Q, Cc	Triangular, irregular, spheritoid, rhombic	1-8	5-15	81, 136, 139, 142, 157, 160, 178
Qiuling						
Au mineralization	Q-PD0-IV, Q-PD7-1 (1)	Q	Irregular, elliptic, negatively crystalline	1-2	5-25	182, 198, 215, 217, 253, 268
Sb mineralization	Q-Tc0-Ca, Q304-7	Q, Cc	Irregular, elliptic, tube-shaped	3-6	5-25	181, 184, 187, 205, 277
Carbonation	Q304-5, Q304-6	Cc	Spheroid, elliptic, elongated, rhombic, irregular	5-8	10-40	149, 153, 161, 184, 212
Yaojian						
Sb mineralization	Y30-1	Q	Fine tube-shaped, elongated	0.5-3	2-25	120, 167
Carbonation	Y40-9	Q	Triangular, irregular, rounded, elongated	0.5-4	4-40	120, 192
Guloushan						
Sb mineralization	D3-5	Q	Elongated, irregular, fibrous	1-3	5-30	142, 144

Note: Compiled from Zhang Fuxin (1997), Zhao Liqing (1997) and the authors' study. Q. Quartz; Cc. calcite.

2.2 Liquid-phase composition

As can be seen from Table 2, the ore-forming fluids are generally characterized by $Cl^- > F^-$ and $Na^+ > K^+$, belonging to the Cl^--Na^+ type. Generally speaking, the contents of F^-, Cl^-, SO_4^{2-}, Na^+ and K^+ in fluid inclusions formed at the Au and Sb mineralization stages are obviously lower than those at later stages, indicating that the ore-forming fluids during the main stage of mineralization are highly capable of dissolving ore-forming materials. During the main stage of mineralization, large amounts of metal minerals were precipitated while they trapped large numbers of fluid inclusions.

In the samples of the same generation, the contents of Na^+, K^+, SO_4^{2-} and Cl^- and the total amounts of anions and cations in quartz inclusions are all higher than those in calcite inclusions, while the case is opposite for Mg^{2+} and F^- (Fig. 3). And SO_4^{2-}/Cl^- ratios in quartz are one order of magnitude lower than those in calcite. The possible explanation is: the existence of quartz implies that the contents of Si-O complex cations are high; in case the concentrations of Si-O complex cations are high, Mg^{2+} can combine with Si-O complex anions to form $MgSiO_4$ and also can be precipitated in the form of Mg-bearing silicate minerals. As a result, the concentrations of Mg^{2+} in hydrothermal solutions could only be kept at low level. On the contrary, Na^+ and K^+ can dissolve in fluids as stable external cations. Meanwhile, F^- can destroy the Si-O bond to form SiF_4 and escapes via evaporation.

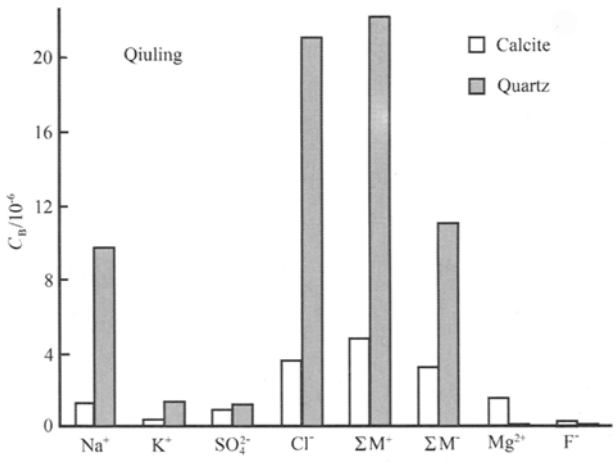

Fig. 3. Comparison of ion concentrations between the inclusions in coexisting calcite and those in quartz (taking Sb mineralization of the Qiuling ore deposit for example).

Therefore, the activity of F^- must be lower than that of Cl^- in the acidic solutions, which have high contents of Si-O complex anions. That is to say, the contents of Cl^- are relatively high. In regard to calcite, its precipitation requires high activities of CO_3^{2-}, Ca^{2+}, Mg^{2+} and other cations and relatively low activities of Si-O complex anions. Lower Si-O complex anionic activities would make F^- exist stably in fluids, leading to the increase of F^- concentrations in the blocked fluids. As the solubility product of $CaCO_3$ was lower than that of $MgCO_3$, the former would be preferentially precipitated, making Mg^{2+} retained in the fluids, thus leading to the increase of Mg^{2+} content in fluid inclusions.

And, owing to the common-ion effects, in case the contents of Mg^{2+} are high, the contents of Na^+ and K^+ would be relatively low in the fluids.

Table 2. Liquid composition of fluid inclusions from the Jindongshan gold ore belt (10^{-6})

Deposit	Sample No.	Stage	Mineral	F^-	Cl^-	SO_4^{2-}	HCO_3^-	Na^+	K^+	Mg^{2+}	Ca^{2+}	$\Sigma M^{-①}$	$\Sigma M^{+②}$	Cl^-/F^-	Na^+/K^+	Remark
Jinlongshan	J-PD52-1	Au	Q	2.23	3.38	12.99	10.37	1.23	18.44	-	-	18.60	19.67	1.52	0.07	*
	J153-1	Au	Q	0.44	49.40	1.85	-	30.88	4.71	0.95	0.00	51.69	36.54	112.27	6.56	* *
	J-PD7-Ca	Sb	Cc	0.89	4.78	53.60	-	2.54	0.38	-	-	59.27	2.92	5.37	6.68	*
	J-mg-3	Carb	Cc	0.35	1.41	1.44	-	0.63	0.33	2.08	-	3.20	3.04	4.03	1.91	
	J-mg-4	Carb	Cc	0.05	0.24	0.29	-	0.28	0.29	1.26	-	0.58	1.83	4.90	0.97	
	J-mg-5	Carb	Cc	0.64	1.35	1.20	-	0.66	0.38	2.42	-	3.19	3.46	2.11	1.74	
Qiuling	Q-PD0-Ⅳ-2	Au	Q	0.04	1.29	2.00	18.31	1.06	1.36	-	-	3.33	2.42	32.25	0.78	*
	Q-PD7-Ca	Sb	Cc	1.40	7.45	Mass	-	3.14	0.49	-	-	Mass	3.63	5.32	6.41	*
	Q304-7	Sb	Cc	0.31	3.56	0.96	-	1.26	0.40	1.57	-	4.83	3.23	11.48	3.15	
	Q304-7	Sb	Q	0.05	21.00	1.20	-	9.67	1.34	0.07	0.62	22.25	11.08	428.57	7.22	
Q304-6(2)	Carb	Cc		0.15	1.30	1.20	-	0.39	0.30	0.72	-	2.65	1.41	8.67	1.30	
Q304-6(5)	Carb	Cc		0.30	1.35	0.72	-	0.74	0.29	1.56	-	2.37	2.59	4.50	2.55	
Yaojian	Y30-1	Au	Q	0.52	25.9	0.62	-	11.47	10.88	0.02	0.00	27.04	22.37	49.81	1.05	* *
	Y36-3-1	Sb	Cc	1.55	4.90	0.44	-	2.19	0.42	1.87	0.00	6.89	4.48	3.16	5.21	* *
Guloushan	D3-4	Au	Q	0.71	24.9	1.85	-	15.44	3.41	0.04	0.00	27.46	18.89	35.07	4.53	* *

Note: Au. Au mineralization; Sb. Sb mineralization; Carb. carbonation; Q. quartz; Cc. calcite. ① The sum of anion and cation concentrations, but HCO_3^- was not taken into account; ② Ca^{2+} was not taken into account. * From Zhang Fuxin et al. (1997); * * from Zhao Liqing (1997); the others were determined by liquid ion gas chromatography (Zhu Heping) at the Mineral Resources Exploration and Research Center under the Institute of Geology and Geophysics, Chinese Academy of Sciences. The analytical instrument is a Japan-made LC-10A Type gas liquid ion gas chromatograph. The relative analytical errors are less than 5%. " - " indicates the values are lower than the detection limit.

From the above it is seen that inclusions in quartz are rich in Na^+, K^+, Cl^-, etc., while those in calcite are rich in Mg^{2+} and F^-. It is worthy of note that the aforementioned differences are still noticed between quartz and ferrodolomite from the Shuangwang gold deposit hosted in the Devonian strata at Qinling (No. 4 in Fig. 1). The contents of SO_4^{2-} in various ore deposits at the main mineralization stage are higher than those at later stages (Table 2), reflecting that the activities of HS^- and S^{2-} in fluids during the mineralization stage are higher than those during later stages. That is because various forms of sulfur were oxidized into SO_4^{2-} in the process of measurement. Precipitation of metallic sulfides in large amounts and large-scale consumption of HS^- and S^{2-} as well as metallic ions in fluids during the main stage of mineralization led to the drastic decrease of those ions in the late-stage fluids, indicating a small contribution to the mineralization during later stages.

The authors conducted laser Raman spectrometric analysis at the Laboratory of Environmental Resources and Lithosphere Dynamic, Petroleum University (Dongying) and found that there commonly existed CO_3^{2-} in fluid inclusions (Fig. 4), demonstrating that the ore-forming fluids would have been derived predominantly from the strata composed mainly of carbonates and clastic rocks.

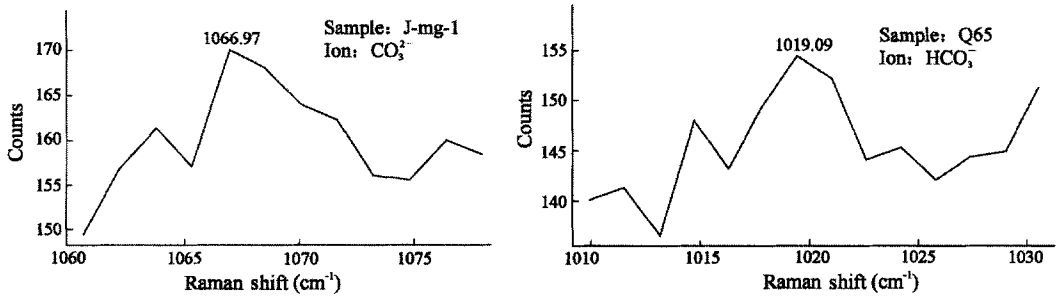

Fig. 4. The laser Raman spectra of CO_3^{2-} and HCO_3^- in fluid inclusions.

Table 3. Gas composition of fluid inclusions from the Jinlongshan gold ore belt (mol%)

Deposit	Sample No.	Stage	Mineral	CH_4	H_2O	CO	N_2	C_2H_6	CO_2	O_2	H_2S	Ar	$\frac{H_2O}{CO_2}$	$\frac{CO_2}{CH_4}$	$\frac{CH_4}{CO}$	$\frac{CO_2}{CO}$	R	Remark
	J-PD52-1	Au	Q	0.221	96.894	0.092	0.209	-	2.583	-	-	-	37.52	11.67	2.40	27.99	0.12	*
	J153-1	Au	Q	0.340	98.630	0.009	0.127	-	0.894	-	-	-	110.35	2.63	38.18	100.37	0.39	**
Jinlongshan	J-PD7-Ca	Sb	Cc	0.060	95.468	0.063	0.421	-	3.988	-	-	-	23.94	66.95	0.94	63.25	0.03	*
	J-mg-3	Carb	Cc	0.361	92.97	-	0.22	0.617	5.575	0.074	0.071	0.112	16.68	15.44	∞	∞	0.06	
	J-mg-4	Carb	Cc	0.294	94.93	0.38	0.221	0.727	3.206	0.079	0.104	0.058	29.61	10.90	0.77	8.44	0.21	
	J-mg-5	Carb	Cc	0.233	94.78	0.096	0.56	0.761	3.227	0.128	0.121	0.093	29.37	13.85	2.43	33.61	0.10	
	Q-PD-Ⅳ-2	Au	Q	0.217	95.807	0.081	0.441	-	3.457	-	-	-	27.72	15.91	2.67	42.49	0.09	*
	Q-PD7-Ca	Sb	Cc	0.274	94.084	0.113	0.188	-	5.341	-	-	-	17.62	19.47	2.44	47.47	0.07	*
	Q304-7	Sb	Q	0.403	93.484	0.549	1.238	0.473	3.482	0.078	0.118	0.175	26.85	8.64	0.73	6.34	0.27	
Qinling	Q304-7	Sb	Cc	0.459	92.577	-	0.063	0.956	5.411	0.052	0.066	0.417	17.11	11.79	∞	∞	0.08	
	Q-CS-7	Sb	Cc	0.384	86.213	-	-	1.996	10.249	0	0.205	0.952	8.41	26.69	∞	∞	0.04	
	Q304-6(2)	Carb	Cc	0.689	74.563	-	0.557	4.492	17.695	0.165	0.212	1.628	4.21	25.68	∞	∞	0.04	
	Q304-6(5)	Carb	Cc	0.523	84.831	-	-	-	14.478	-	0.093	0.075	5.86	27.68	∞	∞	0.04	
Yaojian	Y30-1	Au	Q	0.213	95.497	0.007	0.688	-	3.595	-	-	-	26.56	16.89	31.25	527.73	0.06	**
	Y36-3-1	Sb	Cc	0.023	96.063	0.092	0.050	-	3.772	-	-	-	25.47	164.46	0.25	41.12	0.03	**
Guloushan	D3-4	Au	Q	0.077	98.712	0.016	0.150	-	1.046	-	-	-	94.39	13.64	4.85	66.08	0.09	**

Note: Au. Au mineralization; Sb. Sb mineralization; Carb. carbonation; Q. quartz; Cc. calcite. Reduction parameter $R=(H_2+CO+CH_4)/CO_2$. * From Zhang Fuxin et al. (1997); ** from Zhao Liqing (1997); the others were analyzed using the quadruple mass spectrometric method by Zhu Heping. The instrument is a Japan-made RG202 type one manufactured by the Japanese Vacuum Technology Kabuskiki Kaisha and the working condition: SEM voltage: -1.76 kV; mode of ionization: EI; ionic energy: 50 eV; measuring speed: 50 ms/mau; vacuity: 5×10^{-6} Pa; relative analytical error: <5%; "-" indicates the values are lower than the detection limit.

2.3 Gas-phase composition

The gas-phase composition of fluid inclusions and relevant parameters are listed in Table 3. From the Au, Sb mineralization stage to the carbonation stage the contents of N_2 and CO_2 in fluid inclusions tend to increase. At the carbonation stage there was detected a certain amount of O_2 (Table 3), indicating that with the evolution of mineralization process, the ore-forming fluid system would become more open, and more and more meteoric waters were incorporated into the ore-forming fluids. This implies that the ore-forming depth became shallower and shallower and that in the process of mineralization there occurred crustal uplift.

From early to late, the contents of H_2O in the ore-forming fluids tend to decrease, CO_2 to increase, and H_2O/CO_2 ratios to decrease obviously (Table 3), implicating that the concentrations of CO_2 increased progressively. According to the principle of chemical equilibrium, the ions CO_3^{2-} and HCO_3^- in solutions would also increase. Unfortunately, due to the limitation of analytical technology, the definite concentrations of CO_3^{2-} and HCO_3^- in the solutions have not yet been acquired. However, laser Raman spectrometric analysis has confirmed that there did exist large amounts of the ions CO_3^{2-} and HCO_3^- in fluid inclusions from late samples (Fig. 4). The progressive increase of CO_3^{2-} and HCO_3^-, as described above, reflects the importance of decarbonation in wall-rock alterations, indicating that at the time of fluid/rock interaction, SiO_4^{2-} replaced CO_3^{2-}, hence making more and more CO_2 and CO_3^{2-} find their way into fluids and carbonate minerals in ore-hosting zones progressively. This accords with the tendency of variation of H_2O/CO_2 ratios in the ore-forming fluids producing the Shuangwang and Baguamiao (No. 5 in Fig. 1) gold deposits in the WQGP (Fan Shuocheng and Jin Qinhai, 1994; Wei Longming et al., 1994) and also in consistency with the characteristics of the Carlin-type gold deposits (Kerrich et al., 2000; Berger and Bagby, 1991) and in consistency with the mineral assemblage sequence in the Jinlongshan gold ore belt. Meanwhile, these characteristics also reflect that in the process of mineralization there occurred almost no precise fluid boiling (otherwise, CO_2 would be lost in large amounts owing to fluid boiling). As the source of fluids is relatively shallow and the ore-forming depth is relatively shallow, the ore-forming temperature and pressure are relatively low. In addition, these characteristics are in conflict with the rules of evolution of ore-forming fluids for the orogenic-type gold deposits occurring in greenstone belts and volcanic rocks. Taking the Abitibi gold ore province of Canada (Kerrich and Feng, 1992), the Kalgoorlie gold ore province of Australia (Ho et al., 1990), the Xiaoqinling gold orefield of Henan Province (Xu Jiuhua et

al., 2001), the Shanggong gold deposit of the Xiong'ershan gold orefield (Fan Hongrui et al., 1998), the Kangshan gold deposit (Wang Haihua et al., 2001) and the Tieluping silver deposit (Sui et al., 2000) for example, H_2O/CO_2 ratios in their ore-forming fluids tend to increase from early to late, reflecting that the evolution of ore-forming fluids and ore mineral-assemblage are greatly affected by the characteristics of the wall rocks (Chen Yanjing et al., 1992; Kerrich, 1993; Groves and Foster, 1991).

The contents of C_2H_6 in fluid inclusions are significantly higher than those of CH_4. As viewed from the Jinlongshan and Qiuling gold deposits, the contents of CH_4 and C_2H_6 in late stage inclusions are both higher than those during the Sb mineralization stage. This may be attributed to the higher contents of organic matter in the ore-hosting strata because organic matter can be decomposed through oxidation to generate CH_4, C_2H_6 and CO_2 under the action of ore-forming hydrothermal solutions, thereafter leading to the higher contents of light hydrocarbons in late stages than in the main stage of mineralization. Another reason is that the ore-forming temperature was low during the late stage, favoring the stable existence of C_2H_6.

3 The H-O-C isotopic systematics in ore-forming fluids and its genetic significance

As can be seen from Table 4, the $\delta^{18}O$ values of minerals are within the range of −16.5‰ – +25.5‰, indicative of ^{18}O enrichment, close to the range of $\delta^{18}O$ values for sedimentary rocks (+5‰ – +25‰) (Wei Juying and Wang Guanyu, 1988). The reason may be that the ore-forming fluids came from the country rocks with high $\delta^{18}O$, or they underwent intense isotope exchange with the country rocks. It is known that the Hercynian-Indosinian tectonic strata in the WQGP and ore-hosting rocks are carbonaceous-siliceous mudstone formations; the stratiform siliceous rocks have $\delta^{18}O$ values around 20‰ (Zhang Ligang, 1989), the $\delta^{18}O$ values of cherts in the limestones are within the range of 20.5‰ – 21.4‰, and those of biogenic limestones in the Jinlongshan mining district are 23.4‰. All the data showed that the rocks are capable of providing $\delta^{18}O$-high fluids.

The $\delta^{18}O$ values of the Jinlongshan ore deposit decreased from the Au mineralization stage (24.3‰ – 25.9‰) to the carbonation stage (16.5‰ – 17.9‰). The mineralization temperature tends to decrease as well. Therefore, a decrease in ^{18}O of ore-forming fluids indicates the involvement of more meteoritic waters. From early to late, the δD values of fluid inclusions tend to increase progressively (Table 4).

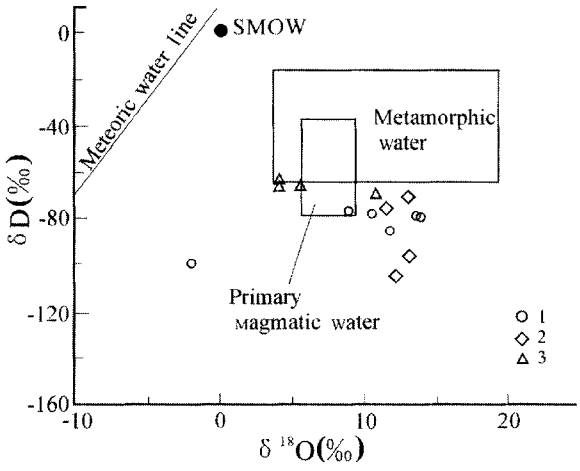

Fig. 5. δD-$\delta^{18}O$ diagram of ore-forming fluids in the Jinlongshan gold ore belt. 1. Au mineralization; 2. Sb mineralization; 3. carbonation. The base chart is after the Open Lab of Ore Deposit Geochemistry, Institute of Geochemistry, Chinese Academy of Sciences (1997).

The average δD value of fluids at the main stage of mineralization of the Jinlongshan ore deposit is −87‰, while −65‰ at the late stage. The δD values for the Qiuling ore deposit vary between −83‰ and −69‰. All these δD values fluctuate near those of local meteoric waters of Mesozoic (J-K) age (δD = −88‰) (Zhang Ligang, 1985). On the δD – $\delta^{18}O$ diagram of ore-forming fluids (Fig. 5) the points of ore-forming fluids fall within the field of magmatic water or on both sides of it, or near the lower boundary of metamorphic water, with the majority of the samples obviously shifting rightwards relative to the meteoric water line, illustrating a full isotopic exchange between the country rocks and the fluids, or the derivation of fluids from the country rocks. As a result, the fluids enriched in $\delta^{18}O$. It is also indicated that the ore-forming fluids appear to have come from meteoric water-source sedimentary formation water. As is shown in Fig. 5, from early to late, the ore-forming fluids showed a tendency of evolution toward meteoric water. The distribution patterns of the points of the Jinlongshan gold ore field on the δD – $\delta^{18}O$ diagram are close to those of the Baguamiao gold deposit (Fig. 1) [the δD and $\delta^{18}O$ values of inclusions in quartz are −117.9‰ – −53.5‰ and −3.1‰ – 13.3‰, respectively (Wei Longming et al., 1994) and the Shuangwang gold deposit (the δD and $\delta^{18}O$ values of inclusions in quartz, calcite and ferrodolomite are −62.2‰ – −131.9‰ and −8.3‰ – 15.2‰, respectively) (Fan Shuocheng and Jin Qinhai, 1994)], and also are approximate to those of the Carlin-type gold deposits of China (Liu Dongsheng et al., 1994).

Table 4. $\delta^{13}C_{PDB}$, δD_{SMOW} and $\delta^{18}O_{SMOW}$ values of minerals and fluid inclusions in the Jinlongshan gold ore belt (‰)

Deposit	Sample No.	Mineralization stage	Mineral	δD_{H_2O}	$\delta^{18}O_{mineral}$	$\delta^{18}O_{H_2O}$	$\delta^{13}C_{fluid}$	$\delta^{13}C_{mineral}$	Remark
Jinlongshan	JPD52-1	Au	Quartz	-79	25.1	13.65	-	-	*
	J153-1	Au	Calcite	-	24.3	-	-	1.5	* *
	J153-2	Au	Quartz	-86	25.9	11.83	-	-	* *
	JPD7-Ca	Sb	Fe-bearing calcite	-97	22.7	13.16	-	-4.0	*
	J-mg-3	Carbonation	Calcite	-66	17.9	5.54	-1.8	0.2	
	J-mg-4	Carbonation	Calcite	-63	16.5	4.14	-3.1	0.8	
	J-mg-5	Carbonation	Calcite	-66	16.5	4.14	-2.8	1.0	
	J112	Country rock	Bio-limestone	-	23.4	-	-	1.5	* *
Qiuling	qPD0-3-2	Au	Quartz	-80	25.3	13.85	-	-	*
	Q64-5	Au	Fe-bearing calcite	-	20.4	-	-	-5.1	* *
	qPD7-Ca	Sb	Calcite	-105	21.8	12.26	-	0.3	*
	Q304-7	Sb	Calcite	-76	22.3	11.64	-1.2	-0.7	
	Q304-7	Sb	Quartz	-71	25.5	13.07	-0.1	-	
	Q304-6-2	Carbonation	Calcite	-69	22.0	10.72	-1.5	-1.6	
	Q304-6-5	Carbonation	Calcite	-69	22.1	10.82	-1.3	-3.6	
Yaojian	Y30-1	Au	Quartz	-77	23.0	8.93	-	-	* *
	Y36-3-1	Sb	Fe-bearing calcite	-100	6.7	-1.85	-	-2.9	* *
	Y36-3-2		Calcite	-	21.8	-	-	-2.6	* *
Guloushan	D3-4	Au	Quartz	-78	24.6	10.53	-	-	* *
	D1-2	Sb	Fe-bearing calcite	-	20.8	-	-	-3.9	* *

Note: $\delta^{18}O_{H_2O}$ is taken as the calculated value. The fractionation equations of quartz & calcite and water are: $1000\ln\alpha_{quartz\text{-}water} = 3.42\times10^{-6}/T^2 - 2.86$ (Zhang Ligang, 1985, 200 - 500℃) and $1000\ln\alpha_{calcite\text{-}water} = 2.78\times10^{-6}/T^2 - 2.89$ (O'Neil, 1969, 0 - 800℃), respectively. The others are all measured values. * From Zhang Fuxin et al. (1997); * * from Zhao Liqing (1997); those unmarked values were measured at the Open Lab of Isotopes, Chinese Academy of Geosciences on a MAT251 mass spectrometer. The analytical precision of carbon and oxygen isotopes is 0.2‰ and that of hydrogen isotopes is 2‰; " - " stands for "not detected".

Moreover, from the studies of the Shuangwang gold deposit we can also see that from early to late, the average δD values of fluid inclusions are -96.0‰ (4 samples), -78.6‰ (6 samples) and -32.6‰ (one sample), respectively (Fan Shuocheng et al., 1994), showing a tendency of progressive increasing; the average $\delta^{18}O$ values of fluid inclusions are 13.9‰, 10.8‰ and -7.63‰, showing a tendency of progressive decreasing. Such a variation tendency is in accord with that of the Jinlongshan gold ore belt. These similar features may be ascribed to the fact that they have the identical geotectonic backgrounds, hence leading to the similar processes of evolution of fluids.

The average $\delta^{13}C_{PDB}$ value of 10 calcite samples is -0.87‰ (Table 4), close to the average value (0.56‰ ± 1.55‰) of marine carbonates determined by Keith and Weber (1964) (From Wei Juying et al., 1988), but slightly lower than that (1.5‰) of biogenic limestones in the mining district, showing a significant difference from the $\delta^{13}C_{PDB}$ values of other forms of carbon in the nature (Hoefs, 1997). All this indicates that the carbon was derived predominantly from the ore-host rock series. In addition, with the exception of Fe-bearing calcite, for either fluid or calcite, their $\delta^{13}C$ values show a tendency of decreasing, to some extent, from early to late. For example, at the Sb mineralization stage the $\delta^{13}C$ values of fluids varied from -0.1‰ to -1.2‰; at the late carbonation stage the equivalent values varied from -1.3‰ to -3.1‰. The decrease of $\delta^{13}C$ may be attributed to the following: 1) formation water in late fluids (including the pent-up brines) was relatively small in volume while meteoric water (bearing atmospheric CO_2) was relatively high; 2) the ore-host rocks commonly contain organic matter (Zhang Fuxin et al., 2000), and the orgamic matter would be oxidized and decomposed to produce ^{12}C-rich CO_2 or CH_4 and C_2H_6 under the action of high f_{O_2} fluids, and the involvement of these products into the fluids would decrease latter's $\delta^{13}C$ values and lead to the simultaneous decrease of $\delta^{13}C$ of hydrothermal calcite. Of these two possible factors, the latter one is in consistency with the characteristics revealed in previous studies on the composition of fluid inclusions, i.e., the contents of CO_2, CH_4, C_2H_4 and O_2 in late fluids increased, displaying that the latter is the main factor that led to the decrease of $\delta^{13}C$ of late fluids and calcite.

As is seen in Table 4, not only the $\delta^{13}C$ values of Fe-bearing calcite are obviously lower than those of calcite, but also its $\delta^{13}C$ and δD values are both lower

than those of contemporaneous quartz or calcite. The reason is that the Fe-O and C-O bonds in Fe-bearing calcite are weaker than the Si-O bond in quartz. That is because Fe^{2+} or C is less capable to combine with ^{18}O or OD^- than Si, thus making the $\delta\,^{18}O$ values of the minerals and the δD values of inclusion water lower than those of quartz. As Fe^{2+} belongs to the transition acid while Ca^{2+} belongs to the hard acid (Dai Anbang and Shen Mengchang, 1979), the former is easier to coordinate with $^{12}C_{16}O_3^{2-}$ while the latter is easier to coordinate with $^{13}C\,^{18}O_3^{2-}$, thus leading to the lower $\delta\,^{18}O$ and $\delta\,^{13}C$ values of Fe-bearing calcite than those of calcite. Therefore, the $\delta\,^{13}C$ values of siderite and Fe-bearing calcite described in this work are so low as to be close to that ($-5‰$) of the initial carbon from the mantle, but it doesn't mean the carbon or ore-forming fluids were derived from the mantle.

4 Conclusions

(1) The Jinlongshan gold ore belt is a typical Carlin-type gold ore belt, where the ore deposits were formed under the action of mesothermal and epithermal fluids. The ore-forming fluids belong to the Na^+-Cl^- type. From the Au and Sb mineralization stages to the late carbonation stage the total amounts of anions and cations in fluid inclusions tend to decrease and the oxidizability of fluids tends to increase progressively; the involvement of meteoric water tends to intensify; the mineralization depth tends to become small progressively; the ore deposits were formed in the process of crustal uplifting and their tectonic settings are similar to those of the orogene-type gold deposits.

(2) Although the ore-forming process and tectonic setting of the Jinlongshan gold ore belt are similar to those of the typical orogene-type gold deposits, fluid/rock interaction and the evolutionary characteristics of ore-forming fluids are different from those of the orogene-type gold deposits hosted in greenstone belts and volcanic terrains. The outstanding feature is: the former's wall-rock alteration is characterized by decarbonation while the latter's by carbonation; the former's ore-forming fluids were derived from shallow levels, as revealed by the progressive increase of CO_2, CO_2/H_2O from early to late, while the latter's from relatively deep levels, as evidenced by the progressive decrease of CO_2, CO_2/H_2O from early to late. The main reason is that the country rock formations are different in nature but not ore-forming mechanism and process are different.

(3) The H, O and C isotope data showed that ore-forming fluids of the Jinlongshan gold ore belt were derived predominantly from formation water and meteoric water confined in the country rock formations, with formation water being dominated at the early stage and meteoric water at the late stage. Higher $\delta\,^{18}O$ and $\delta\,^{13}C$ values of the country rocks led to the higher C and O isotopic values of ore-forming fluids, and further to the higher C and O isotopic values of quartz and carbonate minerals in the ore deposits. The increase of oxygen fugacity of the ore-forming fluids led to the oxidization of organic matter in the country rocks to produce ^{12}C and CO_2 which then would find their way into fluids. As a result, the $\delta\,^{13}C$ values of late calcite and other carbonate minerals and fluids decreased.

(4) The contents of Na^+, K^+, SO_4^{2-} and Cl^- and the total amounts of anions and cations in quartz inclusions are all higher than those of inclusions in the contemporaneously coexisting calcite, but the case is opposite for Mg^{2+} and F^-, which may be attributed, as indicated by the theory of coordination chemistry, to the interactions among different components in the process of fluid action. This implies that the geological fluid processes are very complicated and, therefore, the similarities or differences in nature and composition for fluid inclusions cannot be explained simply by fluid sources or fluid processes.

(5) The $\delta\,^{13}C$ and $\delta\,^{18}O$ values of Fe-bearing calcite and the δD values of inclusions are both lower than those of calcite and quartz, and their $\delta\,^{13}C$ values are approximate to the carbon isotopic composition of the initial carbon in the mantle. Coordination chemical and isotope theoretical analyses revealed that the above data neither reflect the duplicity of fluid sources (e.g. binary mixing), nor their derivation from the mantle or magmas. That is the inevitable result of isotope fractionation among different phases.

Acknowledgements Great thanks are due to the No. 14 Gold Team of the Chinese People's Armed Police Troops for its great support in the fieldwork. The authors are also grateful to Mr. Chen Huayong and Mr. Zhang Zengjie for their help with sample measurement and analysis.

References

Berger B. R. and Bagby W. C. (1991) The geology and origin of Carlin-type gold deposits. In *Gold Metallogeny and Exploration* (ed. R. P. Foster) [C]. pp. 210-248. Blackie, Glasgow and London.

Chen Yanjing and Fu Shigu (1992) *Gold Mineralization in West Henan* [M]. pp. 1-234. Seismological Press, Beijing (in Chinese).

Chen Yanjing, Zhang Jing, Zhang Fuxin, Pirajno F, and Li Chao (2004) Carlin and Carlin-like gold deposits in western Qinling Mountains and their metallogenic time, tectonic setting and model [J]. *Geological Reviews*. **50**, 134-152 (in Chinese with English abstract).

Dai Anbang and Shen Mengchang (1979) *Explanation of Periodic Table*

[M]. pp. 1 - 34. Science and Technology Publishing House of Shanghai, Shanghai.

Fan Hongrui, Xie Yihan, and Wang Yinglan (1998) Fluid-rock interaction during mineralization of the Shanggong structure-controlled alteration-type gold deposit in western Henan Province, central China [J]. *Acta Petrologica Sinica.* **14**, 529 - 541 (in Chinese with English abstract).

Fan Shuocheng and Jin Qinhai (1994) Shuangwang type gold deposits in China. In *Carlin-Type Gold Deposits in China* (eds. Liu Dongsheng et al.) [C]. pp. 254 - 285. Nanjing University Press, Nanjing.

Groves D. I. and Foster R. P. (1991) Archean lode gold deposits. In *Gold Metallogeny and Exploration* [C]. pp. 63 - 103. Blackie, Glasgow and London.

Ho S. E., Groves D. I., and Bennett J. M. (1990) *Gold Deposits of the Archaean Yilgarn Block, Western Australia: Nature, Genesis and Exploration Guides* [M]. pp. 1 - 407. Geology Department and University Extension, University of Western Australia Publication.

Hoefs J. (1997) *Stable Isotope Geochemistry* (3rd ed.) [M]. pp. 1 - 201. Springer-Verlag, Berlin.

Hu Jianmin and Zhang Haishan (1994) The geological characteristics of Jinlongshan microscopic disseminated gold deposit in Shaanxi Province. In *Carlin-Type Gold Deposits in China* (eds. Liu Dongsheng et al.) [C]. pp. 306 - 316. Nanjing University Press, Nanjing (in Chinese).

Kerrich R. (1993) Perspectives on genetic models for lode gold deposits [J]. *Mineralium Deposita.* **28**, 362 - 365.

Kerrich R. and Feng R. (1992) Archean geodynamics and the Abitibi-Pontiac collision: Implications for advection of fluids at transpressive collisional boundaries and the origin of giant quartz vein systems [J]. *Earth Science Reviews.* **32**, 33 - 60.

Kerrich R., Goldfarb R., Groves D. et al. (2000) The characteristics, origins and geodynamic settings of supergiant gold metallogenic provinces [J]. *Science in China* (Series D, supp.). **43**, 1 - 68.

Liu Dongsheng, Tan Yunjin, Wang Jianye et al. (1994) Carlin-type gold deposits in China. In *Carlin-Type (Microfine Disseminated-Type) Gold Deposits in China* [C]. pp. 1 - 38. Nanjing University Press, Nanjing (in Chinese).

O'Neil J. R., Clayton R. N., and Mayade T. K. (1969) Oxygen isotope fractionation in divalent metal carbonates [J]. *Chem. Phys.* **51**, 5547 - 5558.

Open Laboratory of Deposit Geochemistry of Chinese Academy of Science (1997) *Geochemistry of Deposit* [M]. pp. 1 - 538. Geological Publishing House, Beijing (in Chinese).

Sui Y. H., Wang H. H., Gao X. L. et al. (2000) Ore fluid of the Tieluping silver deposit of Henan Province and its illustration of the tectonic model for collisional petrogenesis, metallogenesis and fluidization [J]. *Science in China* (Series D, supp.). **43**, 108 - 121.

Wang Haihua, Chen Yanjing, Gao Xiuli et al. (2001) Isotope geochemistry of Kangshan gold deposit in Henan Province and its illustration of the CPMF model [J]. *Mineral Deposits.* **20**, 190 - 198 (in Chinese with English abstract).

Wei Juying and Wang Guanyu (1988) *Isotope Geochemistry* [M]. pp. 1 - 149. Geological Publishing House, Beijing (in Chinese).

Wei Longming, Cao Yuangui, and Wang Minliang (1994) Geological characteristics and genesis analysis of Baguamiao gold deposit in Shaanxi Province. In *Carlin-Type Gold Deposits in China* (eds. Liu Dongsheng et al.) [C]. pp. 286 - 305. Nanjing University Press, Nanjing (in Chinese).

Xu Jiuhua, Xie Yulin, and Qian Dayi (2001) Compositional features of ore fluids of gold deposits in collision orogenic setting. In *Continental Geodynamics and Metallogenesis* (eds. Chen Yanjing et al.) [C]. pp. 73 - 79. Seismological Press, Beijing (in Chinese).

Zhang Fuxin and Ma Jianqin (1996) Formation of the micro-disseminated strata-bound gold deposits, with special reference to structural evolution, Miliang Area, Zhen'an County, Shaanxi Province, China [J]. *Chinese Journal of Geochemistry.* **15**, 314 - 323.

Zhang Fuxin, Wei Kuanyi, and Ma Jianqin et al. (1997) *Geology and Prospecting of Micro-Disseminated Gold Deposits in the South Qinling* [M]. pp. 75 - 103. Northwest University Press, Xi'an (in Chinese).

Zhang Fuxin, Chen Yanjing, Li C. et al. (2000) Geological and geochemical character and genesis of the Jinlongshan-Qiuling gold deposits in Qinling orogen: Metallogenic mechanism of the Qinling-I pattern Carlin-type gold deposits [J]. *Science in China* (Series D). 43 (supp.), 95 - 107.

Zhang Fuxin and Zhang Jing (2001) The geological-goechemical characters and metallogenic mechanism of Carlin-type gold deposits in Jinlongshan-Qiuling area, Qinling. In *Continental Geodynamics and Metallogenesis* (eds. Chen Yanjing et al.) [C]. pp. 119 - 132. Seismological Press, Beijing (in Chinese).

Zhang Ligang (1985) *The Application of Stable Isotope in Geological Science* [M]. pp. 1 - 267. Science and Technology Publishing House of Shaanxi Province, Xi'an (in Chinese).

Zhang Ligang (1989) *Petrogenetic and Minerogenetic Theories and Prospecting* [M]. pp. 1 - 200. Press of Beijing University of Technology, Beijing (in Chinese).

Zhao Liqing (1997) *Geology, Geochemistry and Metallogeny of Jinlongshan Mineral Belt, East Qinling* (south part) (Ph. D. thesis) [D]. pp. 1 - 97. Department of Geology, Peking University, Beijing (in Chinese).